Citation: Gorbunov, M.E., and G. Kirchengast, Processing X/K Band Radio Occultation Data in Presence of Turbulence: An Overview, in Atmosphere and Climate: Studies by Occultation Methods (U. Foelsche, G. Kirchengast, A.K. Steiner, eds.), pp. 183-192, Springer, Berlin-Heidelberg, 2006.

Processing X/K Band Radio Occultation Data in Presence of Turbulence: An Overview

M. E. Gorbunov[1,2] and G. Kirchengast[2]

[1] Institute of Atmospheric Physics, Moscow, Russia
gorbunov@dkrz.de

[2] Wegener Center for Climate and Global Change (WegCenter) and Institute for Geophysics, Astrophysics, and Meteorology (IGAM), University of Graz, Austria

Abstract. Canonical Transform (CT) and Full-Spectrum Inversion (FSI) methods can be used in processing radio occultation (RO) data to retrieve transmission profiles, which are necessary for the retrieval of atmospheric humidity. LEO-LEO occultations with X/K band frequencies can provide transmission data along the wing of the 22 GHz water vapor absorption line. The retrieval of transmission requires spherical symmetry of the atmospheric refractivity. This condition is broken in presence of turbulence, which can result in significant errors in transmission. We suggest the computation of the differential transmission from the differential CT/FSI-amplitude to correct for the effect of turbulence and horizontal gradients. The efficiency of the method is tested by realistic numerical end-to-end simulations. We modeled turbulence based on power form of the spectrum. The simulations demonstrate that the error in the retrieved transmission can be significant in a single frequency channel, while the differential transmission can be retrieved with high accuracy.

1 Introduction

Radio occultations using GPS signals proved to be a very powerful technique of sounding the Earth's atmosphere [14]. However, atmospheric refractivity indicates very weak absorption and dispersion at GPS frequencies. This makes it impossible to separate the dry and wet terms of the retrieved refractivity without employing additional a priori information. Use of an observation system of Low Earth Orbiters (LEOs) implemented with transmitters and receivers of radio signals in 9 GHz to 30 GHz band can solve this problem [12, 13, 15]. Water vapor has an absorption line centered near 22 GHz. Therefore, from measurements of phase and amplitude, complex refractive index can be retrieved. Then, pressure, temperature, and water vapor profiles can be solved for, using a spectroscopic model of the water vapor line and the hydrostatic equation. [12] describe this retrieval processing in detail, but restricted to the geometric-optics approach for the transmission and bending angle retrieval.

Here the focus is on transmission and bending angle retrieval by wave-optical methods, which will be the approach generally required with real data, since the retrieval scheme will encounter a significant challenge in case of turbulence. The amplitude of a radio occultation signal is significantly more sensitive to small scale turbulence than the phase [16, 17]. In presence of turbulence, the amplitude of the wave field undergoes strong scintillations, which can overwhelm the effect of absorption. In order to reduce the effect of scintillations, it was suggested to use twin frequencies [1, 15].

Given the measurements of the wave field $u_1(t)$ and $u_2(t)$ for two frequencies f_1 and f_2, the difference $\Delta f = f_1 - f_2$ being small enough, we consider the ratio $|u_1(t)| \,/\, |u_2(t)|$. Because for neighbor frequencies the effects of diffraction and interference will not differ significantly, it is expected that they will be reduced in the ratio. The amplitude is proportional to the absorption factor $\exp(-\tau_{1,2})$, where $\tau_{1,2}$ is the integral absorption along a ray for frequency f_1 or f_2. In this case $\ln(u_1(t)/u_2(t))$ equals differential absorption, $\tau_2 - \tau_1$. However, this is only valid for Δf being small enough. On the other hand, choice of too small Δf will result in too low values of the differential absorption, which will increase the noise sensitivity.

The wave optics processing methods such as Canonical Transform (CT) [2, 5, 6, 7] or Full-Spectrum Inversion (FSI) [10, 11] transform the wave field into the representation of impact parameter. In this representation, the amplitude describes the distribution of the energy with respect to impact parameters. For a spherically-symmetric atmosphere, the amplitude of the transformed wave field is proportional to the exponential function of the integral absorption along the ray. Therefore, CT and FSI techniques can be used for the retrieval of atmospheric absorption [3, 11]. These techniques will significantly reduce retrieval errors due to multipath and diffraction. However, the problem of turbulence still persists. Since turbulence is a 3D inhomogeneous structure, the amplitude of the transformed wave field also indicates scintillations [16].

In this study, we suggest the differential method for retrieval of absorption in combination with the CT or FSI techniques. These methods define the transformed wave field $\hat{\Phi} u_{1,2}(p)$, where p is the impact parameter. The transformed field at each single frequency is then to a very significant extent free from the effects of diffraction and multipath. These effects may only be significant for atmospheric inhomogeneities with scales below 50 m [7]. The logarithmic ratio of the transformed amplitudes $\ln\left(\left|\hat{\Phi} u_1(p)\right| / \left|\hat{\Phi} u_2(p)\right|\right)$ will then further suppress the scintillations due to small scale turbulence and will be equal to the differential absorption $\tau_2 - \tau_1$ with a much higher accuracy then the direct amplitude ratio $\ln(|u_1(t)| \,/\, |u_2(t)|)$.

We tested the performance of the new type of the differential method in numerical simulations. In the simulations we used 3D global fields from an ECMWF analysis with superposition of random 2D turbulence. The simulations include modeling realistic receiver noise using the ACE+ baseline values of 67 dBHz.

2 Description of Method

Given measurements of the complex wave field during a radio occultation experiment, $u(t)$, its transform to the representation of the impact parameter is given by the following Fourier Integral Operator (FIO):

$$\hat{\Phi}u = \sqrt{\frac{-ik}{2\pi}} \int a(p,Y) \exp(ikS(p,Y))u(Y(t))\mathrm{d}Y, \tag{1}$$

where $k = 2\pi/\lambda$ is the wavenumber, $a(p,Y)$ and $S(p,Y)$ are the amplitude and phase function of the FIO, respectively, Y is a coordinate along the trajectory, which generalizes the use of coordinate θ in the FSI method [5, 6, 10, 11]. The amplitude function has the following form [6]:

$$a(p,Y) = \left(\sqrt{r_\mathrm{R}^2 - p^2}\sqrt{r_\mathrm{T}^2 - p^2}\frac{r_\mathrm{R} r_\mathrm{T}}{p} \sin\theta\right)^{1/2}. \tag{2}$$

The asymptotic solution for the wave field can be expressed in terms of the inverse FIO with the following amplitude function [6]:

$$a^*(Y,p) = \left(\frac{1}{\sqrt{r_\mathrm{R}^2 - p_\mathrm{R}^2}\sqrt{r_\mathrm{T}^2 - p_\mathrm{T}^2}} \frac{p_\mathrm{T}}{r_\mathrm{R} r_\mathrm{T} \sin\theta} \frac{\mathrm{d}p_\mathrm{T}}{\mathrm{d}p}\right)^{1/2}, \tag{3}$$

where r_T and r_R are (LEO-)Transmitter and (LEO-)Receiver satellite radii, and θ is the angular distance between the satellites, p_T and p_R are the impact parameters at transmitter and receiver satellite, and p is the effective impact parameter.

For a spherically symmetric atmosphere, $p_\mathrm{R} = p_\mathrm{T} = p$. Generally, due to horizontal gradients, these three impact parameters are different, and the following equation can be established [4]:

$$p_\mathrm{R} = p_\mathrm{T} + \int \frac{\partial n}{\partial \theta} \mathrm{d}s, \tag{4}$$

where the integral is taken along the ray. p_R and p_T can be expressed as functions of effective impact parameter p. The relation between p, p_R, and p_T includes the horizontal gradient of refractive index $\partial n/\partial\theta$, which is unknown a priori.

The amplitude of the transformed wave field retrieved by the CT or FSI method equals the following expression:

$$\begin{aligned} A_{1,2}(p) = \bar{A}_{1,2} \frac{\sqrt{r_\mathrm{R}^2 - p^2}\sqrt{r_\mathrm{T}^2 - p^2}}{\sqrt{r_\mathrm{R}^2 - p_\mathrm{R}^2}\sqrt{r_\mathrm{T}^2 - p_\mathrm{T}^2}} \frac{p_\mathrm{T}}{p} \frac{\mathrm{d}p_\mathrm{T}}{\mathrm{d}p} \exp(-\tau_{1,2}(p)) \equiv \\ \equiv \bar{A}_{1,2} K(p) \exp(-\tau_{1,2}(p)). \end{aligned} \tag{5}$$

This expression is represented as a composition of the normalizing constant $\bar{A}_{1,2}$, integral absorption along the ray $\exp(-\tau_{1,2}(p))$, and the factor $K(p)$ that depends on the horizontal gradients. For a spherically layered medium, factor $K(p)$ equals unity, and absorption can be retrieved from the CT amplitude. For a 3D medium with horizontal gradients, factor $K(p)$ approximately equals $\mathrm{d}p_{\mathrm{T}}/\mathrm{d}p$, differing from unity. This shows that in presence of 3D inhomogeneities, in particular, atmospheric turbulence, the amplitude of the transformed wave field, $A_{1,2}(p)$ will undergo scintillations. Since factor $K(p)$ is unknown a priori, the error of the retrieved absorption in each channel will equal $\ln K(p)$.

It is important that $K(p)$ does not depend on the frequency of the wave field. Therefore, the term $\ln K(p)$ will cancel in the differential transmission $\tau_2(p) - \tau_1(p)$ and only some residual diffractive effects will be left. These residual errors are best assessed by numerical simulations as discussed below. The normalizing constants $\bar{A}_{1,2}$ are estimated from the wave field at heights from 25 km to 30 km. The logarithmic ratio of the normalized amplitudes can be expressed as follows:

$$\ln \frac{A_1(p)/\bar{A}_1}{A_2(p)/\bar{A}_2} = \tau_2(p) - \tau_1(p). \tag{6}$$

Here transmissions $\tau_{1,2}(p)$ are measured in Neper. Multiplication with a factor of $20/\ln 10$ will convert them to dB.

The described method is assessed and verified below by rigorous wave optical forward-inverse simulations with fields containing severe small-scale random turbulence and thermal receiver noise.

3 Numerical Simulations

A realistic model of turbulent atmosphere includes regular part from ECMWF analyses and anisotropic turbulence with a magnitude chosen according to radiosonde measurements. Turbulence was modeled as a random anisotropic relative perturbation of the refractivity field with a power form of the spectrum:

$$\tilde{B}(\kappa) = \begin{cases} \tilde{c}\kappa_{\mathrm{ext}}^{-\mu} & \kappa < \kappa_{\mathrm{ext}} \\ \tilde{c}\kappa^{-\mu} & \kappa_{\mathrm{ext}} \le \kappa \le \kappa_{\mathrm{int}} \\ \tilde{c}\kappa^{-\mu} \exp\left[-\left(\dfrac{\kappa - \kappa_{\mathrm{int}}}{\kappa_{\mathrm{int}}/4}\right)^2\right] & \kappa > \kappa_{\mathrm{int}} \end{cases} \tag{7}$$

where $\kappa = \left(\kappa_z^2 + q^2 \dfrac{\kappa_\theta^2}{r_E^2}\right)^{1/2}$, κ_z and κ_θ are the spatial frequencies (wave numbers) conjugated to the polar coordinates z and θ in the occultation plane, q is the anisotropy coefficient [8, 9]. The factor of $\tilde{c}$ normalizes the rms turbulent fluctuations to unity. In the coordinate space we use an additional factor of

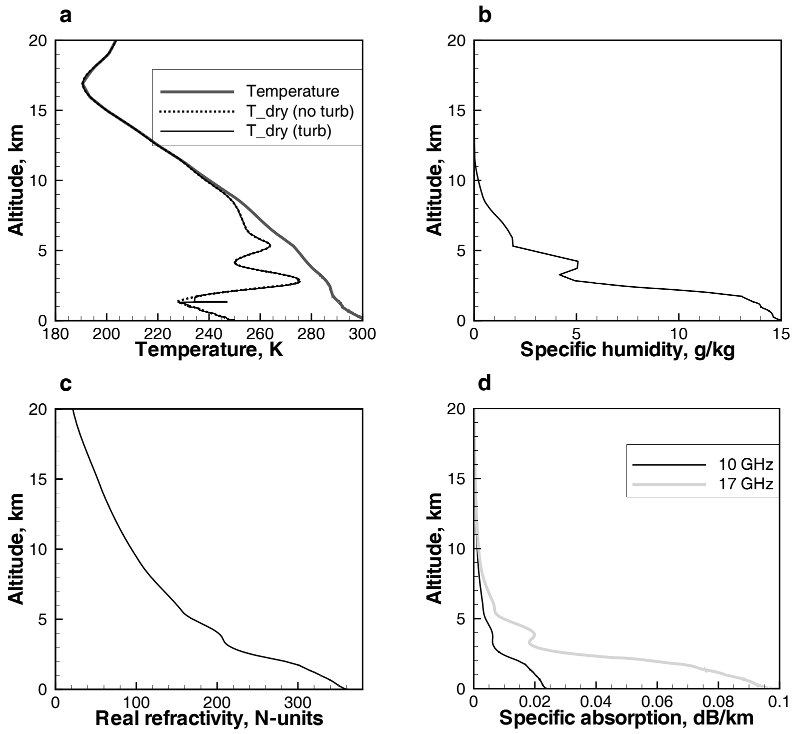

Fig. 1. Simulated occultation event 0118, May 29, 2001, UTC 13:12, 10.4°S 140.7°E, ECMWF field with superimposed power turbulence, frequency channels 10 GHz and 17 GHz: (a) local temperature of the modeled atmosphere T and retrieved dry temperatures, T_{dry} for the regular medium and dry temperature $T_{\mathrm{dry}}^{(\mathrm{turb})}$ for the turbulent medium, (b) specific humidity, q, (c) real refractivity, N, and specific absorptions, $(20/\ln 10)kN_I$, for the two frequencies.

$c(z)$, which describes the relative magnitude of turbulent perturbations as a function of altitude. We performed single-run simulations, because each simulation is a time-consuming procedure, and a montecarlo simulation would require too large a computation time.

Figures 1, 2, and 3 show the results of simulations for a tropical occultation. The turbulence is characterized by external scale $2\pi/\kappa_{\mathrm{ext}} = 0.3$ km, internal scale $2\pi/\kappa_{\mathrm{int}} = 0.03$ km, exponent $\mu = -4$ (-5 for 3D spectrum), and anisotropy $q = 20$. The magnitude $c(z)$ was set according to a low-latitude radiosonde observation on St. Helena island (Stephan Bühler, private communication, 2004): $c(z)$ equals 0.006 at a height of 2.0 km, and logarithmic-linearly decreases to 0.0005 at a height of 7.5 km. Beyond this interval, $c(z)$ is constantly extrapolated. The refraction angle profile indicates strong multipath propagation. The random error of CT differential transmission is about 0.2 dB (4 % to 5 % std.deviation).

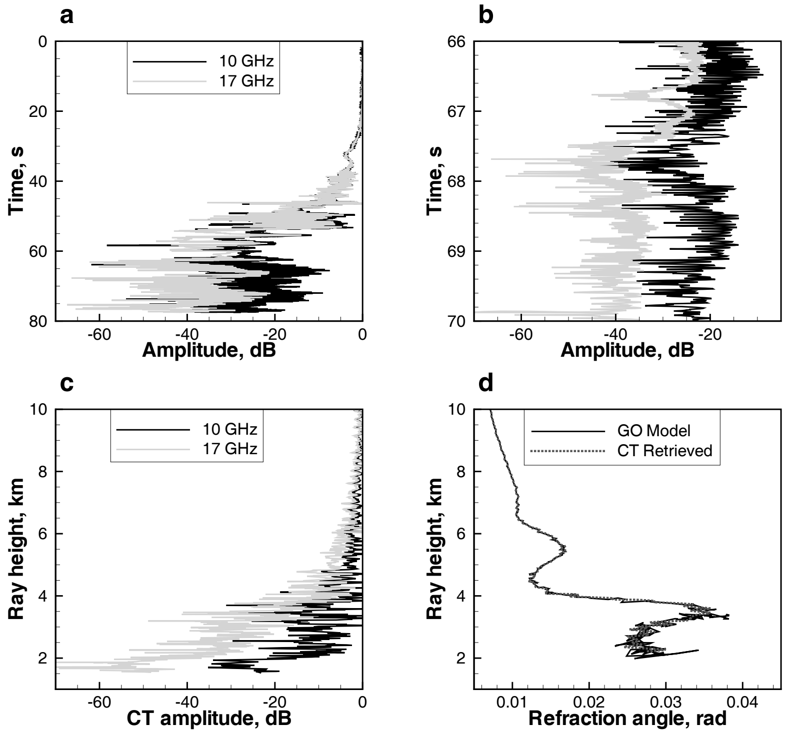

Fig. 2. The same simulated event with superimposed power turbulence, frequency channels 10 GHz and 17 GHz: (a) amplitudes in the two channels, (b) enlarged fragment of amplitude records in multipath area, (c) CT amplitudes for the two channels, and (d) refraction angles, computed by the GO model and retrieved by the CT method.

Figure 4 shows the results of processing the same simulated event with superimposed receiver noise with a magnitude of 67 dBHz. The increase of transmission retrieval errors due to the noise is most visible below a ray height of about 3.5 km, in the area of strong multipath propagation, where the amplitude is low.

4 Conclusions and Outlook

Processing X/K band radio occultation data in presence of turbulence poses a significant challenge, due to the scintillations imposed by the turbulence in the measured amplitude profiles. In earlier transmission retrieval approaches, a possibility was discussed of retrieving differential absorption from the direct ratio of measured amplitudes for two different (closely spaced) frequency

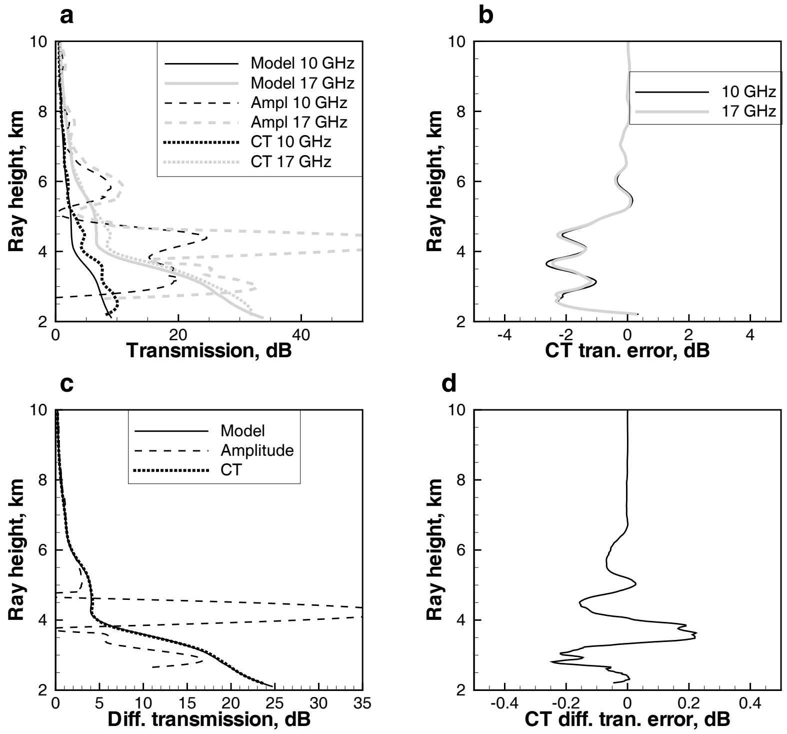

Fig. 3. The same simulated event with superimposed power turbulence, frequency channels 10 GHz and 17 GHz: (a) transmissions for the two channels, true model, computed from the amplitudes, and computed from the CT amplitudes, (b) errors of the CT transmission, (c) differential transmission, true model, computed from the measured amplitudes $|u_{1,2}(t)|$, and computed from the CT amplitudes, and (d) errors of the CT differential transmission.

channels. Here we discussed an advanced differential method of retrieval of atmospheric transmissions based on the ratio of the CT amplitudes.

The new method results in much more accurate correction for turbulence scintillations, as compared to taking the direct ratio of the measured wave fields. This is due to the following reasons: 1) The CT mapping corrects for diffraction and multipath propagation effects, 2) The resulting transformed field is independent from diffraction except for small scales below about 50 m. 3) The ratio of the transformed amplitudes then further corrects for small-scale scintillations and effects of the non-sphericity of the atmosphere. 4) The new method does not impose any significant restriction for the frequency difference Δf between the channels, and there is no requirement that Δf is small (e.g., clearly smaller than 1 GHz). This has important technical advantages and provides very good differential transmission sensitivity if spacings of a few GHz are chosen (e.g., 10 GHz and 17 GHz or 17 GHz and 20 GHz, or similar).

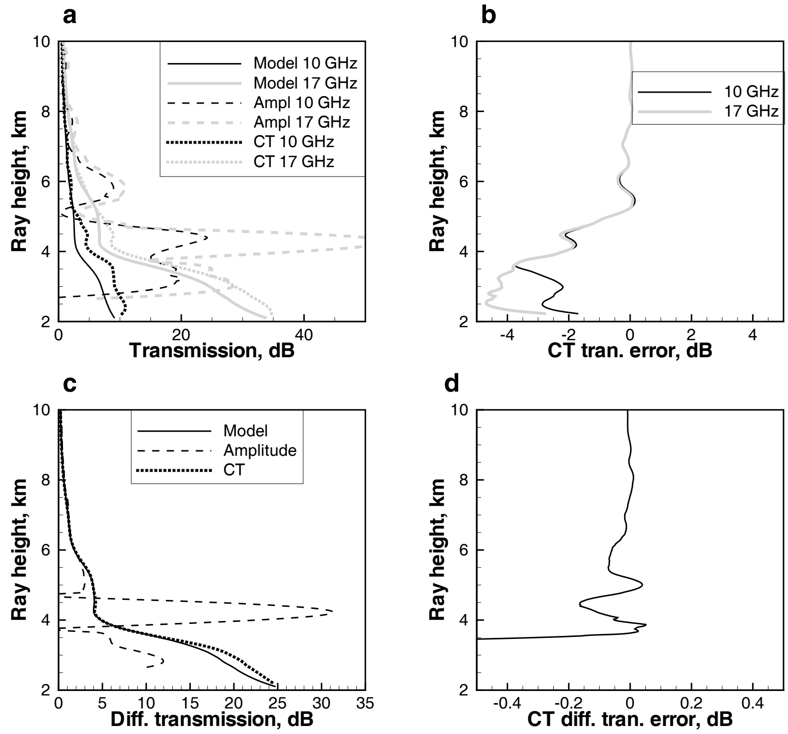

Fig. 4. The same simulated event with superimposed power turbulence, frequency channels 10 GHz and 17 GHz, with a model of receiver noise 67 dBHz: (a) transmissions for the two channels, true model, computed from the amplitudes, and computed from the CT amplitudes, (b) errors of the CT transmission, (c) differential transmission, true model, computed from the measured amplitudes $|u_{1,2}(t)|$, and computed from the CT amplitudes, and (d) errors of the CT differential transmission.

In practice the frequency separation is limited by a finite SNR and the large attenuation for the 22 GHz line, which broadens out in the lower troposphere. Using more frequencies may then be required to limit the dynamic range.

We performed numerical simulations with a realistic model of the turbulent atmospheric refractivity field in a rigorous forward-inverse modeling framework. The model also included receiver noise at a realistic level (carrier-to-noise 67 dBHz, ACE+ baseline). These numerical simulations showed the high capabilities of the CT differential method. The influence of the noise is only significant below a ray impact height of 4 km (below 2 km to 3 km altitude), where the carrier-to-noise ratio is becoming very low due to strong absorption and defocusing in the lower troposphere. In this context 1 kHz sampling rate is the minimum required rate for adequate wave optics processing of X/K band occultation data. Effects of small amplitude drifts of 0.5 % over

20 s (ACE+ specification for maximum drift) were also assessed and found of minor relevance compared to thermal noise and of no further concern.

Processing differential transmissions further to imaginary refractivity and, in turn, together with real refractivity derived from bending angles, to atmospheric profiles is a procedure identical to using single-channel transmissions [12, 13, 15]. Due to the differencing, there is one differential transmission profile less, however, than single-channel transmission profiles. In the case of ACE+ with 3 frequencies this implies availability of two differential transmission profiles, which are still sufficient in combination with the real refractivity profile to separate water vapor and liquid water from temperature, down into the lower troposphere.

Further efforts to perform the explicit turbulence modeling at higher resolution (e.g., down to inner scale of turbulence of 10 m instead of 30 m, and down to an-isotropy coefficients as small as 5) will be worthwhile, for assessment of the theoretical expectation that residual errors will become smaller when approaching isotropic turbulence.

Independent of such further work, there is clear evidence from the present study already that in those turbulent cases, where single-channel transmissions might be too noisy to be processed directly, the use of differential transmissions is an adequate alternative. It can be expected, based on the experience from single-channel transmission processing [13], that also differential transmissions will allow to meet X/K band occultation observation requirements such as laid out for ACE+.

Acknowledgements. The authors gratefully acknowledge valuable discussions related to this work with A.S. Gurvich (IAP Moscow, Russia), S.V. Sokolovskiy (UCAR, Boulder, CO, USA), F. Cuccoli (Univ. of Florence, Italy), S. Buehler (Univ. of Bremen, Germany), P. Silvestrin (ESA/ESTEC, Noordwijk, Netherlands), and further colleagues of the ESA-ACEPASS study team. The work was funded by ESA under ESTEC Contract No. 16743/02/NL/FF.

References

[1] Facheris L, Cuccoli F (2003) Analysis of differential spectral attenuation measurements applied to a LEO-LEO link. ESA-ACEPASS Report (contract 16743/02/NL/FF), Inst of Elect and Telecommunications, Univ of Florence

[2] Gorbunov ME (2002) Canonical transform method for processing radio occultation data in lower troposphere. Radio Sci 37(5), doi:10.1029/2000RS002592

[3] Gorbunov ME (2002) Radio-holographic analysis of Microlab-1 radio occultation data in the lower troposphere. Journal of Geophysical Research 107, doi:10.1029/2001JD000889

[4] Gorbunov ME, Kornblueh L (2001) Analysis and validation of GPS/MET radio occultation data. Journal of Geophysical Research 106:17 161–17 169

[5] Gorbunov ME, Lauritsen KB (2002) Canonical transform methods for radio occultation data. Scientific Report 02-10, Danish Meteorological Institute, Copenhagen, Denmark, http://www.dmi.dk/dmi/Sr02-10.pdf

[6] Gorbunov ME, Lauritsen KB (2004) Analysis of wave fields by Fourier Integral Operators and its application for radio occultations. Radio Sci 39(4), RS4010, doi:10.1029/2003RS002971

[7] Gorbunov ME, Benzon H-H, Jensen AS, Lohmann MS, Nielsen AS (2004) Comparative analysis of radio occultation processing approaches based on Fourier integral operators. Radio Sci 39(6), RS6004, doi:10.1029/2003RS002916

[8] Gurvich AS, Brekhovskikh VL (2001) Study of the turbulence and inner waves in the stratosphere based on the observations of stellar scintillations from space: A model of scintillation spectra. Waves in Random Media 11, 163–181, doi:10.1088/0959-7174/11/3/302

[9] Gurvich AS, Chunchuzov IP (2005) Estimates of characteristic scales in the spectrum of internal waves in the stratosphere obtained from space observations of stellar scintillations. J Geophys Res 110(D3), D03114, doi:10.1029/2004JD005199

[10] Jensen AS, Lohmann MS, Benzon H-H, Nielsen AS (2003) Full spectrum inversion of radio occultation signals. Radio Sci 38, doi:10.1029/2002RS002763

[11] Jensen AS, Lohmann MS, Nielsen AS, Benzon H-H (2004) Geometrical optics phase matching of radio occultation signals. Radio Sci 39(3), RS3009, doi:10.1029/2003RS002899

[12] Kirchengast G, Fritzer J, Schwaerz M, Schweitzer S, Kornblueh L (2004) The atmosphere and climate explorer mission ACE+: Scientific algorithms and performance overview. Tech Report for ESA/ESTEC No 2/2004, Inst for Geophys, Astrophys, and Meteorol, Univ of Graz, Austria

[13] Kirchengast G, Schweitzer S, Ramsauer J, Fritzer J, Schwaerz M (2004) Atmospheric profiles retrieved from ACE+ LEO-LEO occultation data: Statistical performance analysis using geometric optics processing. Tech Report for ESA/ESTEC No 1/2004, Inst for Geophys, Astrophys, and Meteorol, Univ of Graz, Austria

[14] Kursinski ER, Hajj GA, Leroy SS, Herman B (2000) The GPS radio occultation technique. Terrestr Atmosph Ocean Sci 11(1):53–114

[15] Kursinski ER, Syndergaard S, Flittner D, Feng D, Hajj G, Herman B, Ward D, Yunck T (2002) A microwave occultation observing system optimized to characterize atmospheric water, temperature and geopotential via absorption. Journal of Atmospheric and Oceanic Technology 19(12):1897–1914

[16] Sokolovskiy SV (2001), Tracking tropospheric radio occultation signals from low earth orbi. Radio Sci 36(3):483–498, doi:10.1029/1999RS002305

[17] Yakovlev OI, Matyugov SS, Vilkov IA (1995) Attenuation and scintillation of radio waves in the Earth's atmosphere from radio occultation experiment on satellite-to-satellite links. Radio Science 30(3):591–602